Modulation of Endocrine Pancreas Development but not β-Cell Carcinogenesis by Sprouty4

Fabienne Jäggi,[1] Miguel A. Cabrita,[1] Anne-Karina T. Perl,[2] and Gerhard Christofori[1]

[1]Institute of Biochemistry and Genetics, Department of Clinical-Biological Sciences, Center of Biomedicine, University of Basel, Basel, Switzerland and [2]Division of Pulmonary Biology, Cincinnati Children's Hospital Medical Center, Cincinnati, Ohio

Abstract

Sprouty (Spry) proteins modulate signal transduction pathways elicited by receptor tyrosine kinases (RTK). Depending on cell type and the particular RTK, Spry proteins exert dual functions: They can either repress RTK-mediated signaling pathways, mainly by interfering with the Ras/Raf/mitogen-activated protein kinase pathway or sustaining RTK signal transduction, for example by sequestering the E3 ubiquitin-ligase c-Cbl and thus preventing ubiquitylation, internalization, and degradation of RTKs. Here, by the inducible expression of murine Spry4 in pancreatic β cells, we have assessed the functional role of Spry proteins in the development of pancreatic islets of Langerhans in normal mice and in the Rip1Tag2 transgenic mouse model of β-cell carcinogenesis. β cell–specific expression of mSpry4 provokes a significant reduction in islet size, an increased number of α cells per islet area, and impaired islet cell type segregation. Functional analysis of islet cell differentiation in cultured PANC-1 cells shows that mSpry4 represses adhesion and migration of differentiating pancreatic endocrine cells, most likely by affecting the subcellular localization of the protein tyrosine phosphatase PTP1B. In contrast, transgenic expression of mSpry4 during β-cell carcinogenesis does not significantly affect tumor outgrowth and progression to tumor malignancy. Rather, tumor cells seem to escape mSpry4 transgene expression. (Mol Cancer Res 2008;6(3):468–82)

Introduction

Receptor tyrosine kinases (RTK) activate signal transduction pathways that control a variety of processes in multicellular organisms, such as proliferation, differentiation, migration, and survival. To ensure a physiologically appropriate biological outcome, the precise spatial and temporal regulation of these signaling pathways is crucial. An effective mechanism of modulation is the evolution of negative-feedback loops, that is, the transcriptional induction of negative regulators by the same pathway that will be eventually inhibited. The Sprouty (Spry) proteins represent one such family of negative regulators of RTK signaling (1-3).

Spry was identified in *Drosophila* as a novel antagonist of fibroblast growth factor (FGF) receptor (FGFR; ref. 4) and epidermal growth factor receptor signaling pathways (5). The mammalian genome contains four *Spry* genes (*Spry1-Spry4*) encoding proteins of 32 to 34 kDa (6-9). Similar to the Spry protein in *Drosophila*, all four mammalian isoforms were shown to attenuate the activation of the Ras-Raf-p42/44 extracellular-regulated kinase (p42/44 ERK) pathway induced by various growth factors, including FGF, vascular endothelial growth factor, hepatocyte growth factor, platelet-derived growth factor, insulin, nerve growth factor, and glial cell line–derived neurotrophic growth factor (9-18). Surprisingly, in some cases, Spry proteins fail to repress epidermal growth factor signaling; they even potentiate the activation of this pathway, for example, by the sequestration of the E3 ubiquitin ligase c-Cbl and the prevention of RTK ubiquitylation, internalization, and degradation (9, 18-22). These data suggest that in vertebrates, Spry proteins are not simply general inhibitors of RTK signaling but rather selective modulators of different RTK pathways (23, 24). The four mammalian Spry proteins contain a conserved cysteine-rich COOH-terminal domain and variable NH_2-terminal domains and interact with a variety of signaling molecules, including c-Cbl, CIN85, Grb2, c-Raf, Frs2, TESK, caveolin-1, and Gap1 (1-3). Other proteins have been implicated in interacting with Spry proteins [e.g., Src or protein-tyrosine phosphatase-1B (PTP1B)], but these have not been conclusively shown (25-27). Hence, multiple mechanisms exist by which Spry proteins interfere with RTK signaling, depending on the cellular context, the identity of the RTK, or the Spry isoform.

In adult tissues, Spry1, Spry2, and Spry4 are widely expressed (6-8), whereas Spry3 expression is restricted to brain and testis (8). However, the regulation of Spry expression and the functional consequences of Spry activity in adult tissues have not been extensively characterized. During development and organogenesis, the expression pattern of Spry strongly overlaps with known sites of RTK signaling. For example, in the developing zebrafish, Spry4 expression is dependent on FGF8 and FGF3 signaling and antagonizes pathways activated by FGFR1 (28). In mammals, embryonic tissues, such as brain, heart, gut, lung, and muscle, show a close spatial and temporal

Received 6/5/07; revised 11/3/07; accepted 11/13/07.
Grant support: Swiss National Science Foundation grants SNF 3100-068133 and 3100A0-109574 (G. Christofori), and a postdoctoral fellowship from the IARC-WHO (M.A. Cabrita).
The costs of publication of this article were defrayed in part by the payment of page charges. This article must therefore be hereby marked *advertisement* in accordance with 18 U.S.C. Section 1734 solely to indicate this fact.
Requests for reprints: Gerhard Christofori, Institute of Biochemistry and Genetics, Department of Clinical Biological Sciences, Center of Biomedicine, University of Basel, Mattenstrasse 28, 4058 Basel, Switzerland. Phone: 41-61-267-35-64; Fax: 41-61-267-35-66. E-mail: gerhard.christofori@unibas.ch

doi:10.1158/1541-7786.MCR-07-0255

interdependence between FGF signaling and Spry gene expression (8, 29). Loss-of-function analyses in mice confirm the importance of Spry expression for normal development of several organs. Spry1 is an essential antagonist of glial cell line–derived neurotrophic growth factor signaling during kidney induction by regulating morphogenesis of the ureteric epithelium (12). Spry2 is a negative regulator of glial cell line–derived neurotrophic growth factor in the development of enteric nerve cells (11) and it regulates FGF-dependent cell fate transformation in the auditory epithelium, and, when ablated, results in hearing loss (13). Moreover, Spry2 and Spry4 are responsible for restricting FGF-mediated cross talk between the epithelium and mesenchyme during tooth development (30). Likewise, ectopic expression of Spry proteins strongly affects the development of different organs. In chicken, constitutive expression of Spry2 and Spry4 results in the repression of FGF-mediated limb development (8) and forced expression of Spry2 or Spry4 in epithelial cells of the murine fetal lung severely affects lung growth and branching morphogenesis (31, 32). Finally, Spry2 interferes with testis development by inhibiting FGF-driven mesonephric cell migration (33).

Here, we have investigated the functional effect of murine Spry4 (mSpry4) on the development of the endocrine pancreas. Development of the pancreas initiates in the anterior midgut region of the endoderm epithelium. As development proceeds, endocrine precursor cells delaminate from the pancreatic epithelium, migrate into the surrounding mesenchyme, and aggregate into islets of Langerhans—a process requiring cell migration, sorting, and aggregation (34, 35). However, it is not until several weeks after birth that the pancreas fully matures and islets of Langerhans are established with their distinctive cellular architecture: Non-β cells (α, γ, and PP cells expressing glucagon, somatostatin, and pancreatic polypeptide) are localized in the periphery of islets of Langerhans, whereas β cells reside in the center. Studies of pancreas development in mice and rats revealed an important function for FGF signaling in the development of the pancreas (36-42). In adult mice, FGFR1 and FGFR2 together with their ligands FGF1, FGF2, FGF4, FGF5, FGF7, and FGF10 are exclusively expressed in β cells of the endocrine pancreas, indicating that FGF signaling may also have a role in differentiated β cells. Indeed, expression of a dominant-negative version of FGFR1 in β cells affects the organization of endocrine cells within the islets of Langerhans, reduces the number of β cells, and impairs glucose homeostasis (39). Here, we show that the expression of mouse Spry4 in β cells during islet development impairs islet architecture and the sorting of α and β cells.

Because initiation and progression of most, if not all, cancer types are associated with a dysregulation of RTK signaling pathways, Spry proteins may exert critical roles in tumorigenesis via their modulatory functions. Indeed, the expression of Spry1 and Spry2 has been found down-regulated in a variety of cancer types, including cancers of the breast, prostate, and liver and in melanoma cell lines (3, 43-46). In addition, melanomas harboring activating mutations of B-Raf are resistant to growth inhibition by Spry2 because the mutated form of Raf no longer binds to Spry2 (46). However, the functional implications of Spry expression on tumor growth has remained elusive. Hence, in a second set of experiments, we have explored the role of Spry proteins during tumorigenesis by the inducible expression of mSpry4 in a transgenic mouse model of pancreatic β-cell carcinogenesis (Rip1Tag2). In this mouse model, the expression of the SV40 large T antigen in pancreatic β cells leads to the development of β-cell carcinoma through multiple stages, including early hyperplasia, angiogenic hyperplasia, adenoma, and, finally, carcinoma (47-50). These experiments reveal that mSpry4 does not significantly affect T antigen–mediated β-cell carcinogenesis, implicating molecular changes that help to overcome Spry-specific, growth-repressive functions on tumor cells.

Results

Pancreatic Endocrine α Cells Express mSpry4

To determine if endogenous mSpry proteins were expressed by cells of the murine pancreas, we stained sections from pancreata of adult C57Bl/6 mice for all four mSpry isoforms with the corresponding anti-mSpry antisera. No expression was detectable for mSpry1, mSpry2, and mSpry3 by any cell type of the mouse pancreas (data not shown). In contrast, endogenous mSpry4 was found expressed in a subset of cells in the islets of Langerhans (Fig. 1A and B). The localization of these mSpry4-positive cells in the outer rim of the islet was reminiscent of the localization of α cells. Immunofluorescence costaining using antibodies against glucagon as markers for α cells and anti-mSpry4 sera confirmed that endogenous mSpry4 was exclusively expressed in α cells of the islets of Langerhans (Fig. 1C-E).

Transgenic Expression of mSpry4 in β Cells Perturbs Islet Organization

Because several members of the FGF family of growth factors and their receptors are expressed in pancreatic β cells, we assessed the effect of β cell–specific mSpry4 expression on islet development. To this end, doxycycline-inducible $(tetO)_7$mSpry4 transgenic mice (32) were crossed with transgenic mice in which the rat insulin promoter (Rip1) controls synthesis of the reverse doxycycline transactivator (Rip1rtTA; ref. 51). Ectopic mSpry4 protein was readily detected in β cells of adult double-transgenic Rip1rtTA;$(tetO)_7$mSpry4 mice treated with doxycycline for 2 weeks (Fig. 2A). In single transgenic littermates, endogenous mSpry4 expression is only found in α cells but not in β cells as also shown above for nontransgenic C57Bl/6 mice (Fig. 1 and data not shown). In the absence of doxycycline, double-transgenic Rip1rtTA;$(tetO)_7$mSpry4 mice exhibited a weak expression of mSpry4 in β cells, indicating low activity of the doxycycline-inducible promoter even in the absence of doxycycline (Fig. 2B).

Development of the endocrine pancreas starts with pancreatic precursor cells of the duct epithelium invading the surrounding mesenchyme (52, 53). At around E17.5, the first immature islets are found with ongoing segregation of endocrine cells (i.e., β cells in the center and non-β cells in the periphery; refs. 54, 55). To induce mSpry4 expression in developing β cells of the embryos, pregnant females were treated from the day of conception with doxycycline. Because the insulin promoter driving reverse tetracycline transactivator in Rip7rtTA mice is active with the first appearance of insulin-producing endocrine cells (E9-10), mSpry4 is thus expressed

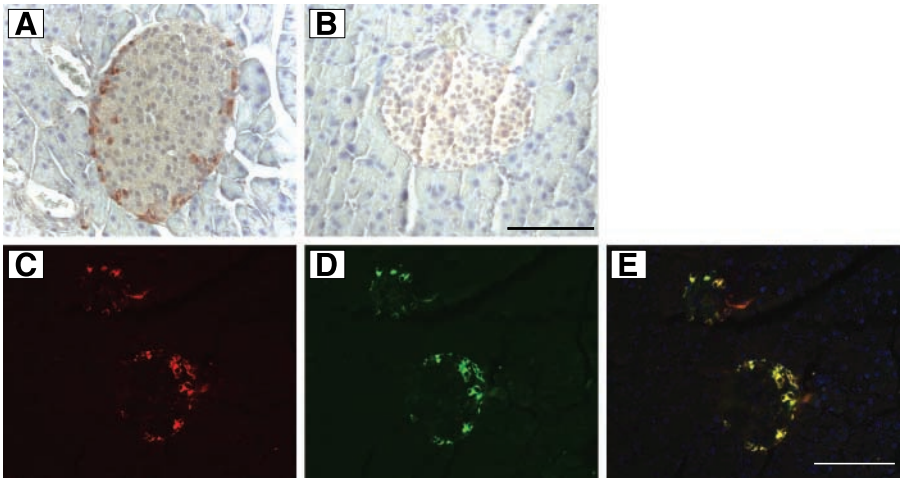

FIGURE 1. mSpry4 expression in pancreata of adult C57Bl/6 mice. Immunohistochemical staining (*brown*) of pancreatic sections from an adult C57Bl/6 mouse using anti-mSpry4 antisera (**A**) or preimmune sera (**B**). Immunofluorescence staining of a pancreatic section from adult C57Bl/6 mouse for the α-cell marker glucagon (**C**; *red*) and for mSpry4 (**D**; *green*). Note that mSpry4 and glucagon are coexpressed in the same cells (**E**; *merge, yellow*). Scale bars, 100 μm.

early during islet development. Costainings for mSpry4 and for the β-cell marker insulin by immunofluorescence revealed the inducibility of the transgene in β cells of embryos, for example at E19.5 (Fig. 2). Single-transgenic control animals expressed endogenous mSpry4 in α cells surrounding insulin-positive β cells (Fig. 2C-E). In pancreata of doxycycline-treated double-transgenic animals, the number of mSpry4-positive cells was substantially increased (Fig. 2F), indicating the induction of β cell–specific mSpry4 expression during embryogenesis. However, the area of insulin-positive cells and the levels of insulin expression were decreased in double-transgenic mice (Fig. 2G; Table 1). In fact, only a small number of β cells coexpressed mSpry4 and insulin, and within these, insulin levels were reduced (Fig. 2H-K).

To analyze α- and β-cell distribution in the developing pancreas, we costained for insulin and glucagon expression in pancreata of E19.5 double-transgenic Rip1rtTA;$(tetO)_7$mSpry4 and single-transgenic mice. In control embryos, a large part of the endocrine pancreas was already organized into normal islets of Langerhans with glucagon-expressing α cells surrounding insulin-positive β cells (Fig. 2L). Such well-structured islets were not observed in doxycycline-induced Rip1rtTA;$(tetO)_7$mSpry4 mice (Fig. 2M). The average islet size in these embryos was significantly reduced at E19.5 compared with islets of littermate controls; the area of insulin-expressing β cells per islet area was decreased; whereas the number of α cells was increased (Table 1). These results indicate that β cell–specific expression of mSpry4 during development dramatically changes islet morphology and α- and β-cell contribution.

We wondered whether the observed difference in islet architecture represented a delay in development that is compensated for at later stages of pancreas formation. Therefore, analysis of islet morphology was done in pancreata of older animals; in 2-week-old pups (PN 14), the process of cell segregation is still ongoing whereas in 4-week-old mice (PN 28), islet formation is complete (54). mSpry4 expression was induced with doxycycline throughout the embryonic development and postnatal life in Rip1rtTA;$(tetO)_7$mSpry4 mice. In agreement with the results of E19.5 pancreata, a significant reduction in islet size in mSpry4-expressing embryos was also observed at the age of 2 weeks (Table 1). In contrast, there was no significant difference in islet size between Rip1rtTA;$(tetO)_7$mSpry4 and control littermates at the age of 4 weeks. The area of insulin-positive cells and the levels of insulin expression were decreased and the proportion of α cells per islet area was significantly increased at both time points. To determine the influence of mSpry4 on islet cell type segregation, we quantified the number of missorted α cells (i.e., α cells that were localized centrally to the two most peripheral cell layers of the islet). Only a few missorted α cells were found in islets of 2-week-old and, to a lesser extent, of 4-week-old control mice (Fig. 2N, *arrow*; Table 1). However, in both age groups analyzed, the number of missorted α cells was significantly higher in mSpry4-expressing Rip1rtTA;$(tetO)_7$mSpry4 mice (Fig. 2O; Table 1). When mice were treated with doxycycline starting only after birth and sacrificed at 4 weeks of age, islet architecture in these mice showed a significant increase in the amount of total α cells and in the number of missorted α cells (data not shown). We found that this phenotype is fully penetrant. Furthermore, glucose tolerance tests revealed that the phenotype in islet architecture caused by mSpry4 expression does not affect glucose metabolism in 5-week-old mice (Supplementary Fig. S1). From these data, we conclude that the presence of mSpry4 in β cells does not result in a major defect of pancreas development but impairs islet cell sorting during all stages of endocrine pancreas development.

mSpry4 Inhibits Migration and Adhesion without Affecting p42/44 ERK Activation

Human pancreatic PANC-1 cells have been used as a useful model to study early stages of pancreatic endocrine islet formation (56, 57). Grown in normal serum–containing medium, PANC-1 cells form an epithelioid, adherent monolayer. When cultured in defined serum-free medium, the cells begin forming islet-like cell aggregates that differentiate into cells expressing markers of the endocrine pancreas, such as insulin, glucagon, or somatostatin (56). This process is strongly dependent on FGF signaling, whereby FGF2 expressed by PANC-1 cells serves as a chemoattractant to induce migration and aggregation of these cells into islet-like cell aggregates (56). Thus, we considered PANC-1 cells a suitable model to assess mSpry4 function during islet formation on a cellular

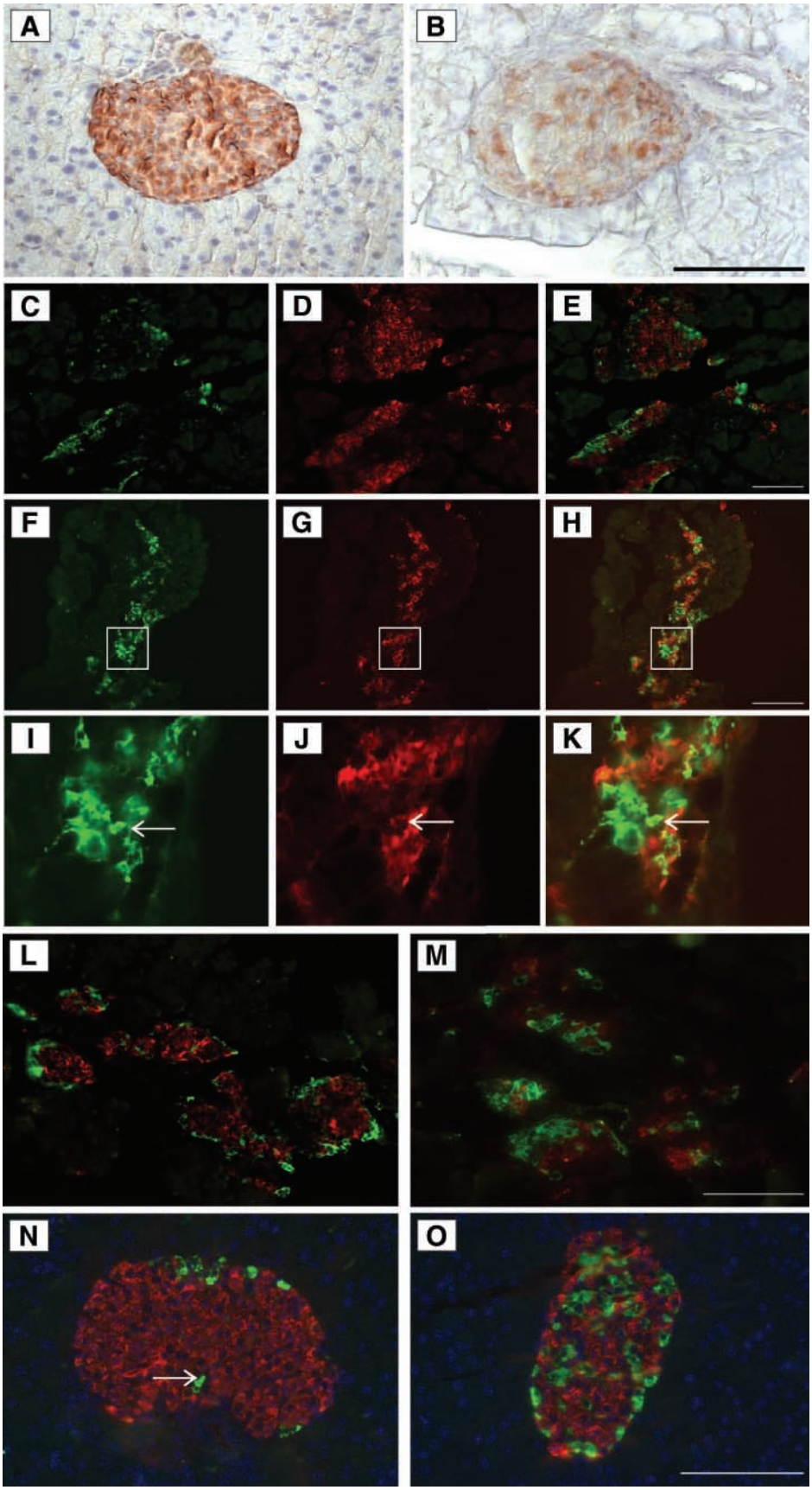

FIGURE 2. Transgenic mSpry4 expression in β cells. Immunohistochemical staining of pancreatic sections from adult Rip1rtTA;$(tetO)_7$mSpry4 mice treated with doxycycline for 2 wk (**A**) or not treated at all (**B**) using anti-mSpry4 antisera (*brown*). Histologic sections of developing pancreas of mouse embryos at E19.5 from single or non-transgenic control littermates (**C**-**E**) and double-transgenic Rip1rtTA;$(tetO)_7$mSpry4 mice (**F**-**H**). Immunofluorescent costaining using anti-mSpry4 sera (**C** and **F**; *green*) and antibodies against the β-cell marker insulin (**D** and **G**; *red*). Merged pictures (**E** and **H**; *yellow*). **I** to **K.** Higher-magnification view of boxed areas indicated in **F** to **H**. Arrows, cells expressing high levels of mSpry4 and low levels of insulin. **L** to **O.** Analysis of islet architecture using immunofluorescent costaining with antibodies against glucagon (*green*) and insulin (*red*). Pancreas of embryos at E19.5 (**L** and **M**) and of 4-wk-old mice (**N** and **O**) from doxycycline-treated single or non-transgenic control mice (**L** and **N**) and from Rip1rtTA;$(tetO)_7$mSpry4 littermates (**M** and **O**). Arrow in **N**, a cell localized centrally to the two most peripheral cell layers. Scale bars, 100 μm.

level. For this purpose, PANC-1 cells were infected with adenovirus encoding mSpry4 (AdmSpry4) or luciferase as control (AdLite). Adenovirus-mediated expression of mSpry4 in these cells was confirmed by immunoblot analysis (data not shown).

To assess whether mSpry4 can interfere with cell migration of PANC-1 cells, Transwell migration assays were done. In serum-free medium, PANC-1 cells did not migrate (data not shown). The presence of 10% FCS in the medium induced migration of PANC-1 cells, which was significantly inhibited by the expression of mSpry4 (Fig. 3A). Inhibitory effects of Spry4 on directed cell movement was assessed by supplementing the medium in the lower Transwell chamber with 10% FCS or with 100 ng/mL FGF2. In accordance with previously published data, where FGF2 in the lower chamber serves as a strong chemoattractant for PANC-1 cells (56), mSpry4 efficiently repressed such serum- and FGF2-induced directional cell migration (Fig. 3A). However, Spry4-expressing cells, but not control-virus–infected cells, underwent apoptosis after 4 to 5 days of culture, thus excluding any long-term analysis (data not shown).

Previously, it has been shown that the formation of islet-like cell aggregates is initiated by brief exposure of PANC-1 cells to low concentrations of trypsin followed by incubation in serum-free medium, suggesting that PANC-1 cells cluster together by paracrine chemotaxis via FGF2 (56). In the presence of mSpry4, the capacity of PANC-1 cells to migrate after brief trypsin exposure was significantly reduced (Fig. 3A). Cell-cell and cell-matrix adhesion also plays an important role in cell type segregation in organ development (58) and thus may affect the formation of islets of Langerhans. When analyzed for adhesion to uncoated versus collagen IV–coated tissue culture plates, mSpry4 strongly inhibited adhesion of PANC-1 cells to both (Fig. 3B). Together, these data indicate that mSpry4 is a general inhibitor of PANC-1 adhesion and motility, which does not discriminate between chemokinesis (nondirectional, random movement) and chemotaxis (directional movement).

Next, we assessed whether the inhibitory effects of mSpry4 on migration and adhesion were achieved by attenuation of p42/44 ERK activation. PANC-1 cells were infected with AdmSpry4 or AdLite, starved overnight, and stimulated with various growth factors known to induce p42/44 ERK activation. Notably, mSpry4 had no effect on pp42/44 ERK levels for any of the activated signaling pathways (Fig. 3C). These data suggest that mSpry4 inhibits adhesion and migration of PANC-1 cells by a mechanism that either acts downstream of p42/44 ERK activation or independently thereof.

mSpry4 Expression Interferes with the Localization of PTP1B

Previously, Spry proteins have been reported as inhibitors of cell migration (25-27), with PTP1B, a phosphatase known to be involved in integrin signaling (59, 60), as a critical mediator of the antimigratory actions of Spry2 (27). We therefore analyzed PTP1B levels in lysates of PANC-1 cells infected with AdmSpry4 or AdLite. Expression of mSpry4 in these cells led to an increase in the levels of PTP1B in the soluble fraction of cell lysates with a concomitant decrease of PTP1B levels in the cell fraction that is insoluble in Triton X-100 (Fig. 4A), suggesting that mSpry4 modulates the subcellular localization of PTP1B.

Immunofluorescence stainings of cells grown on uncoated coverslips revealed that PTP1B in AdLite control-infected PANC-1 cells localized in a pattern typical for proteins that were associated with the endoplasmic reticulum (Fig. 4B; ref. 61). In contrast, in mSpry4-expressing PANC-1 cells, PTP1B was distributed throughout the cytosol (Fig. 4C). When grown on coverslips coated with collagen IV, control cells showed a concentration of PTP1B at punctate structures in the margins of the cells (Fig. 4D), identified previously as cell matrix adhesion sites (61). In contrast, the expression of mSpry4 mostly perturbed the localization of PTP1B (Fig. 4E). As shown by phalloidin/actin staining, mSpry4 did not affect the cytoskeletal organization of the cells (Fig. 4F and G), excluding the possibility that the effect of mSpry4 on PTP1B localization was due to general changes in cytoskeletal architecture.

These results raise the possibility that mSpry4 attenuates migration and adhesion of PANC-1 cells by perturbing the correct localization of PTP1B and thereby interfering with

TABLE 1. Effects of mSpry4 Expression on Islet Development

Age	E19.5		2 wk		4 wk	
Dox treatment	E_0-$E_{19.5}$		E_0-PN_{14}		E_0-PN_{28}	
	Control*	mSpry4 †	Control*	mSpry4 †	Control*	mSpry4 †
Islet area (μm^2)	3,924 ± 316	2,930 ± 267	6,636 ± 503	4,731 ± 412	9,766 ± 1,042	7,617 ± 718
P	0.0004		0.0185		0.0788	
α Cells/area (per 1,000 μm^2)	3.91 ± 0.19	5.1 ± 0.31	5.48 ± 0.26	6.97 ± 0.39	2.76 ± 0.25	4.22 ± 0.57
P	0.0053		0.0037		0.0151	
Insulin-positive area/total islet area (%)	57 ± 2	36 ± 3	56 ± 2	28 ± 2	68 ± 3	57 ± 2
P	0.0001		0.0001		0.0056	
Missorted α cells/islet area (per 1,000 μm^2)	NA		1.5 ± 0.13	2.94 ± 0.26	0.86 ± 0.12	1.92 ± 0.3
P			0.0001		0.0003	
	n = 121	*n* = 132	*n* = 117	*n* = 64	*n* = 54	*n* = 64
	N = 9	N = 13	N = 6	N = 7	N = 6	N = 12

NOTE: Values represent mean ± SD. *P* value of mSpry4 vs control (two-tailed Mann Whitney test). *n*, number of islets; *N*, number of mice.
Abbreviations: Dox, doxycycline; NA, not applicable.
*Rip1rtTA or $(tetO)_7$mSpry4.
†Rip1rtTA;$(tetO)_7$mSpry4.

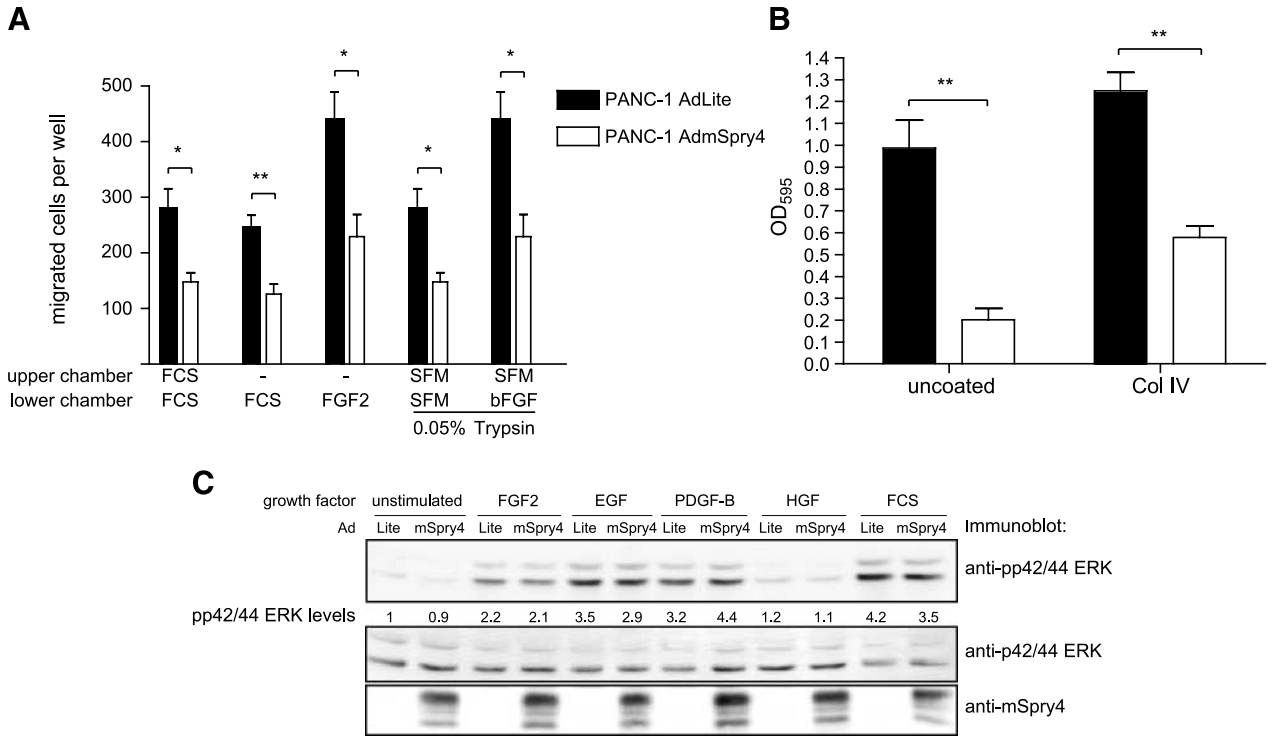

FIGURE 3. mSpry4 inhibits migration and adhesion of PANC-1 cells. **A.** Migration assay. PANC-1 cells infected with AdmSpry4 or control virus (AdLite) were seeded on 8-μm pore size Transwell inserts. The medium in the upper and/or lower chambers was supplemented with 10% FCS or 100 ng/mL FGF2 as indicated. Cells treated with trypsin were exposed to low levels of trypsin after 3 h of adhesion to the Transwell membrane and incubated for another 4.5 h in serum-free medium (*SFM*) alone or with 100 ng/mL FGF2 in the lower chamber as indicated. Columns, mean; bars, SD; representative of four replicates. The graph is representative of two independent experiments. *, $P < 0.05$; **, $P < 0.01$ (Student's *t* test, two-tailed). **B.** Adhesion assay. PANC-1 cells infected with AdmSpry4 or with control virus (AdLite) were seeded on collagen IV (*Col IV*). After 2.5 h, unattached cells were washed off with PBS. Attached cells were fixed, stained with crystal violet, lysed, and absorbance was measured at A_{595}. Columns, mean; bars, SD; representative of four replicates. The graph is representative of two independent experiments. *, $P < 0.05$; **, $P < 0.01$ (Student's *t* test, two-tailed). **C.** Growth factor stimulation. Cells infected with AdmSpry4 or control virus (AdLite) were starved overnight and then stimulated for 30 min with FGF2, epidermal growth factor (*EGF*), platelet-derived growth factor-B (*PDGF-B*), hepatocyte growth factor (*HGF*), or with medium supplemented with 10% FCS as indicated. Lysates were resolved by SDS-PAGE and resulting immunoblots were sequentially probed with anti-phosphorylated p42/44 ERK and anti-total p42/44 ERK antibodies before visualization and quantification with an Odyssey imager. Levels of phospho-p42/44 ERK were normalized against total p42/44 ERK levels. The immunoblot shown is representative of three independent experiments.

integrin function (25, 26). Applying the PANC-1 cell system as a model for islet formation, we hypothesize that this inhibitory function of mSpry might play an important role in migration and sorting of endocrine cells during pancreas development, as observed by the expression mSpry4 *in vivo*.

mSpry4 Expression during Pancreatic β-Cell Carcinogenesis

To investigate the functional role of mSpry4 in tumor development, we used Rip1Tag2 mice, a well-characterized transgenic mouse model of pancreatic β-cell carcinogenesis, and determined the role of ectopic expression of mSpry4 in β-cell tumor development in Rip1Tag2;Rip1rtTA;$(tetO)_7$mSpry4 triple-transgenic mice. Expression of the transgene was induced by doxycycline at different stages of tumorigenesis: (*a*) from week 5 to 8 (initiation of tumorigenesis); (*b*) from week 7 to 10 (tumor outgrowth); and (*c*) from week 10 to 12 (progression from benign to malignant tumors). Littermates negative for either of the transgenes [Rip1rtTA or $(tetO)_7$mSpry4 or both] were used as controls.

Inducible mSpry4 expression in islets and tumors was analyzed by immunoblotting analysis of pooled tumor lysates (Fig. 5A) and by immunohistochemical staining of pancreatic sections using anti-mSpry4 sera (Fig. 5B-E). In pancreata of 8-week-old Rip1Tag2 tumor mice, most islets were still comparable in size and morphology with islets of C57Bl/6 mice, with α cells in the islet periphery expressing endogenous mSpry4 (Fig. 5B). In Rip1Tag2;Rip1rtTA;$(tetO)_7$mSpry4 mice, transgenic mSpry4 expression was induced by doxycycline in β cells of small and hyperplastic islets of 8-week-old (Fig. 5C) and 12-week-old triple-transgenic mice (Fig. 5D). However, the number of cells expressing the transgene markedly declined in adenomas and carcinomas of 10- and 12-week-old mice, in which large areas of the tumors were negative for mSpry4 expression (Fig. 5E; Table 2). Costaining for mSpry4 and insulin by immunofluorescence revealed that the expression of the two proteins was not concomitantly lost, indicating that the reduced mSpry4 expression is not due to a loss of insulin promoter activity (data not shown). In addition, upon analysis of ERK phosphorylation in the pooled tumor lysates (Fig. 5A), the effect of mSpry4 expression on p42/44 ERK activation was variable. In some cases, mSpry4 moderately attenuated ERK activation, reflecting the heterogeneity of mSpry4 expression in these tumors. We therefore conclude that a selection against

mSpry4 expression or against cells expressing mSpry4 occurs during tumor progression.

To assess whether mSpry4 expression in β cells has any effect on tumor incidence or tumor size, isolated pancreata from 10- and 12-week-old Rip1Tag2;Rip1rtTA;$(tetO)_7$mSpry4 mice and from control littermates were analyzed macroscopically. Total numbers of tumors per mouse were not affected by ectopic mSpry4 expression, and a small, and not significant, reduction in tumor volumes was observed in triple-transgenic mice versus control littermates (Table 3). These results suggest that although mSpry4 is not affecting the onset of tumorigenesis, it has a slight effect on tumor growth. Quantification of tumor cell proliferation by bromodeoxyuridine (BrdUrd) incorporation assays revealed that in all three cohorts, the proliferation rate of cells was slightly decreased in tumors expressing transgenic mSpry4 compared with tumors of control mice (Table 3). Analysis of tumor cell apoptosis by terminal deoxyribonucleotide transferase–mediated nick-end labeling (TUNEL) assays revealed a significant decrease in apoptosis only in tumors of 8-week-old Rip1Tag2;Rip1rtTA;tetOPmSpry4 mice compared with tumors of control littermates, whereas there was no difference in tumor cell apoptosis in 10-week-old mice and only a slight, yet not significant, increase in 12-week-old mice (Table 3). Double-immunofluorescence staining by TUNEL assay and with anti-mSpry4 antibodies did not reveal any correlation between mSpry4 expression and apoptosis within individual cells (data not shown), suggesting that mSpry4-expressing cells are not more prone to cell death than cells without mSpry4 expression.

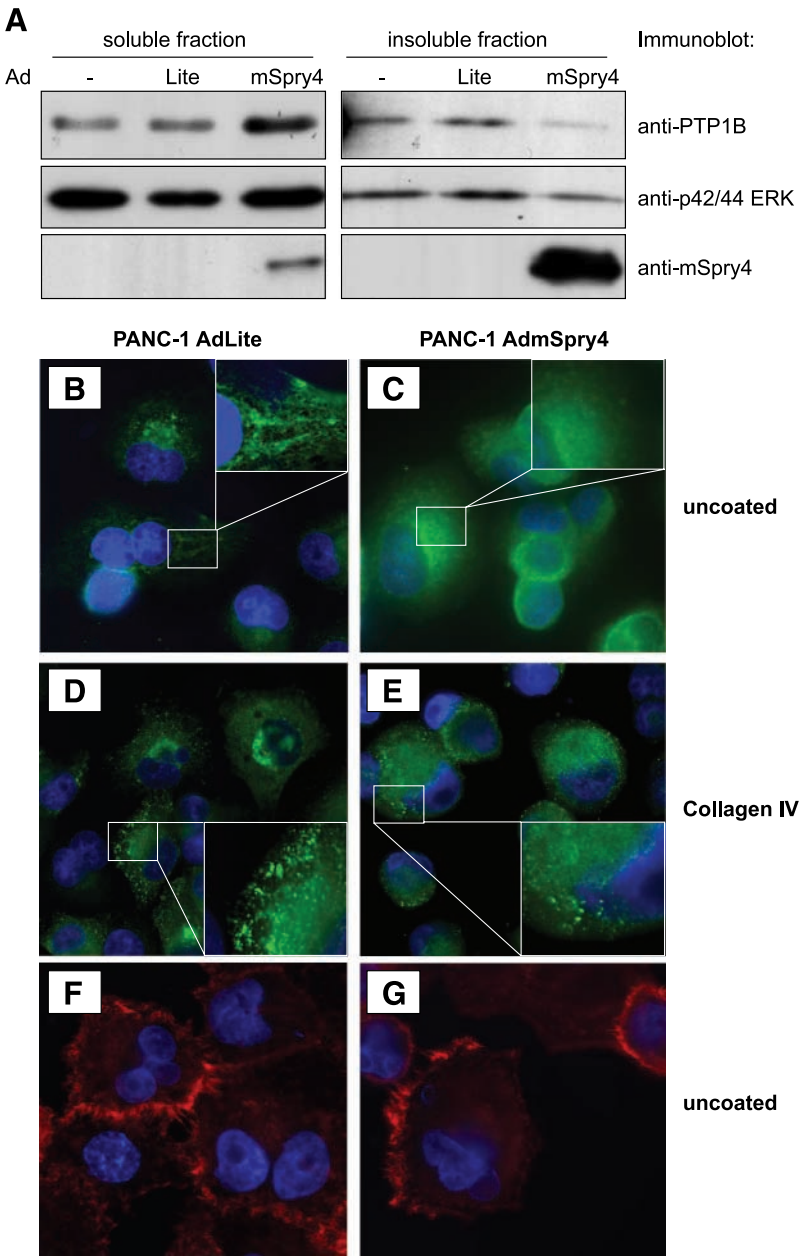

FIGURE 4. Changes of PTP1B localization in PANC-1 cells by the expression of mSpry4. **A.** Triton X-100–soluble and Triton X-100–insoluble fractions of control PANC-1 cells or PANC-1 cells infected with control virus (AdLite) or with AdmSpry4 were resolved by SDS-PAGE, and resulting immunoblots were sequentially probed with the antibodies indicated. Immunofluorescence staining of PANC-1 cells using anti-PTP1B antibodies. Cells infected with control virus AdLite (**B** and **D**) or with AdmSpry4 (**C** and **E**) were grown on glass coverslips (uncoated **B-C**) or on coverslips coated with collagen IV (**D-E**). Visualization of the actin cytoskeleton using phalloidin staining in PANC-1 cells infected with AdLite (**F**) or with AdmSpry4 (**G**).

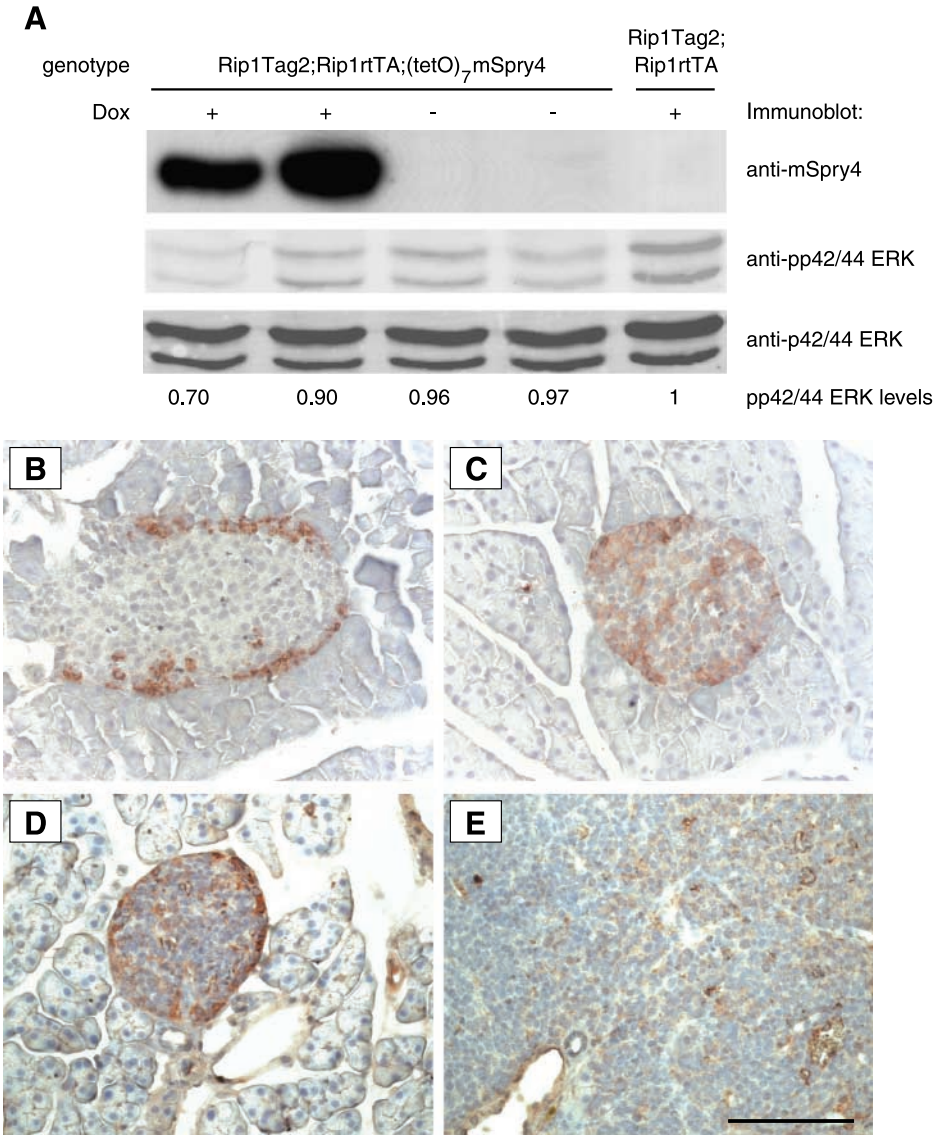

FIGURE 5. Inducible mSpry4 expression in β-cell tumors of Rip1Tag2 mice. **A.** Immunoblotting analysis of lysates from pooled tumors (3-5 mm in diameter) from 12-wk-old Rip1Tag2;Rip1rtTA and Rip1Tag2;Rip1rtTA;$(tetO)_7$mSpry4 mice treated with doxycycline for 2 wk or left untreated as indicated. Equal amounts (50 μg) of lysates were resolved by SDS-PAGE and immunoblots were first probed with anti-mSpry4 antisera and then simultaneously probed with anti-phosphorylated p42/44 ERK and anti-total p42/44 ERK antibodies before visualization and quantitation with an Odyssey imager. Levels of phospho-p42/44 ERK were normalized against total p42/44 ERK levels. Immunohistochemical staining of histologic pancreatic sections from Rip1Tag2 and Rip1Tag2;Rip1rtTA;$(tetO)_7$mSpry4 mice using anti-mSpry4 antisera (*brown*). Islets of a 7-wk-old Rip1Tag2 (**B**) and Rip1Tag2; Rip1rtTA;$(tetO)_7$mSpry4 mice (**C**) after 3 wk of doxycycline treatment. Islet (**D**) and large carcinoma (**E**) of a 12-wk-old Rip1Tag2;Rip1rtTA;$(tetO)_7$mSpry4 mouse after 2 wk of doxycycline treatment. Scale bar, 100 μm.

To test for the possibility that transgenic mSpry4 expression could repress tumor progression, tumors were staged according to their histology into normal/hyperplastic islets, adenomas, and carcinomas of three grades with increasing malignancy (62). No differences in tumor progression between Rip1Tag2;Rip1rtTA;$(tetO)_7$mSpry4 mice and control littermates were observed at any time point (Table 4).

Together, the data indicate that expression of mSpry4 in β tumor cells only moderately impairs tumor growth by modestly repressing tumor cell proliferation. However, β tumor cells seem to select against the expression of mSpry4.

No Effect of mSpry4 on Tumorigenicity of Cultured β Tumor Cells

To investigate the effect of mSpry4 on tumor growth at a cellular level, we established several independent β tumor cell lines from tumors of Rip1Tag2;Rip1rtTA;$(tetO)_7$mSpry4 mice and control littermates. Inducible high expression of mSpry4

TABLE 2. mSpry4 Expression in Developing Tumors

	Normal/Hyperplastic Islets	Adenoma	Carcinoma
Area of mSpry4-expressing cells/tumor area (%)	55.4 ± 7.2	31.2 ± 8.5	3.3 ± 1.5
*P**	0.0447		0.0209
	$n = 9$	$n = 9$	$n = 6$

NOTE: Tumors are from Rip1Tag2;Rip1rtTA;$(tetO)_7$mSpry4 mice. Values represent mean ± SD. n, number of islets/tumors.
*P value of normal/hyperplastic islets vs adenoma and adenoma vs carcinoma (two-tailed Student's t test).

TABLE 3. Expression of mSpry4 Does Not Significantly Affect β-Cell Carcinogenesis

Age	8 wk		10 wk		12 wk	
Dox treatment	Week 5-8		Week 7-10		Week 10-12	
	Control*	mSpry4†	Control*	mSpry4†	Control*	mSpry4†
Tumor incidence/mouse	NA		5.1 ± 1.1 (N = 12)	4.8 ± 1.4 (N = 10)	7.1 ± 0.8 (N = 11)	8.7 ± 1.6 (N = 7)
P			0.8767		0.3321	
Total tumor volume/mouse (μm³)	NA		13.4 ± 4.8 (N = 12)	10.2 ± 4.9 (N = 10)	78.3 ± 17.8 (N = 7)	45.3 ± 18.0 (N = 11)
P			0.6464		0.2344	
Proliferation rate of tumor cells‡	85.0 ± 4.7 n = 70 N = 9	73.6 ± 5.5 n = 53 N = 7	93.2 ± 5.0 n = 74 N = 9	88.2 ± 4.6 n = 72 N = 8	83.7 ± 8.4 n = 41 N = 5	73.1 ± 3.9 n = 99 N = 12
P	0.1168		0.4593		0.1958	
Apoptotic tumor cells§	13.4 ± 0.8 n = 81 N = 11	9.9 ± 0.8 n = 57 N = 7	18.8 ± 1.0 n = 89 N = 11	17.2 ± 1.6 n = 43 N = 6	13.9 ± 0.7 n = 50 N = 8	16.0 ± 0.9 n = 75 N = 9
P	0.0035		0.3813		0.0698	

NOTE: Values represent mean ± SD. P value of mSpry4 vs. control (two-tailed Student's t test). n, number of ×40 microscopic fields. N, number of mice.
*Rip1Tag2/Rip1Tag2;Rip1rtTA/Rip1Tag2;(tetO)$_7$mSpry4.
†Rip1Tag2;Rip1rtTA;(tetO)$_7$mSpry4.
‡Number of BrdUrd-positive cells per ×40 microscopic field.
§Number of TUNEL-positive cells per ×40 microscopic field.

in β tumor cell lines isolated from triple-transgenic animals was confirmed by immunoblotting analysis (Fig. 6A). In contrast to the moderate repression of proliferation in β tumor cells *in vivo* (Table 3), the expression of mSpry4 had no effect on β tumor cell proliferation *in vitro* (Fig. 6B).

To test whether mSpry4 could inhibit p42/44 ERK activation in cultured β tumor cells, β tumor cell lines from Rip1Tag2;Rip1rtTA;(tetO)$_7$mSpry4 mice were cultured in the presence and absence of doxycycline for 2 days to induce mSpry4 expression and were stimulated with different growth factors under starvation conditions. Immunoblotting analysis of the phosphorylation status of p42/44 ERK revealed that ERK signaling was constitutively activated in all cell lines that could not be further stimulated by any of the growth factors tested (Fig. 6C). Notably, in contrast to the heterogeneity of mSpry4 activity observed in the pooled tumors (Fig. 5A), mSpry4 expression in the various tumor cell lines isolated could not attenuate phosphorylation of p42/44 ERK, independent of starvation or stimulation with different growth factors.

Finally, we investigated whether mSpry4 could affect the tumorigenic potential of cultured β tumor cells. Rip1Tag2;Rip1rtTA;(tetO)$_7$mSpry4 β tumor cells were injected s.c. into the flanks of immunodeficient nu/nu mice; one cohort of mice was subsequently treated with doxycycline in the drinking water. Inspection of tumor growth over the course of 6 weeks revealed that there was no significant difference in growth of the transplanted tumors in the presence or absence of mSpry4 expression (Table 5). Taken together, these results show that growth and tumorigenicity of cultured β tumor cells, initially transformed by SV40 T antigen, is not affected by mSpry4 expression.

Discussion

In this study, we have investigated the effect of transgenic mSpry4 expression in β cells in islet development and β-cell tumorigenesis. We show that endogenous mSpry4 is exclusively expressed in α cells of the developing and adult

TABLE 4. Expression of mSpry4 Does Not Affect β-Cell Tumor Progression

Age	8 wk		10 wk		12 wk	
Dox treatment	Week 5-8		Week 7-10		Week 10-12	
	Control*	mSpry4†	Control*	mSpry4†	Control*	mSpry4†
Normal/hyperplastic islets	62	62	34	38	32	35
Adenoma	19	18	21	21	20	20
	81	**80**	**55**	**59**	**52**	**55**
Carcinoma						
G1	15	16	16	16	15	14
G2	3	3	27	22	31	30
G3	1	1	2	3	2	1
	19	**20**	**45**	**41**	**48**	**45**
	n = 213 N = 11	n = 217 N = 9	n = 219 N = 11	n = 224 N = 10	n = 161 N = 12	n = 218 N = 12

NOTE: Values are given as percentage of total tumors. n, number of islets/tumors; N, number of mice.
*Rip1Tag2/Rip1Tag2;Rip1rtTA/Rip1Tag2;(tetO)7mSpry4.
†Rip1Tag2;Rip1rtTA;(tetO)7mSpry4.

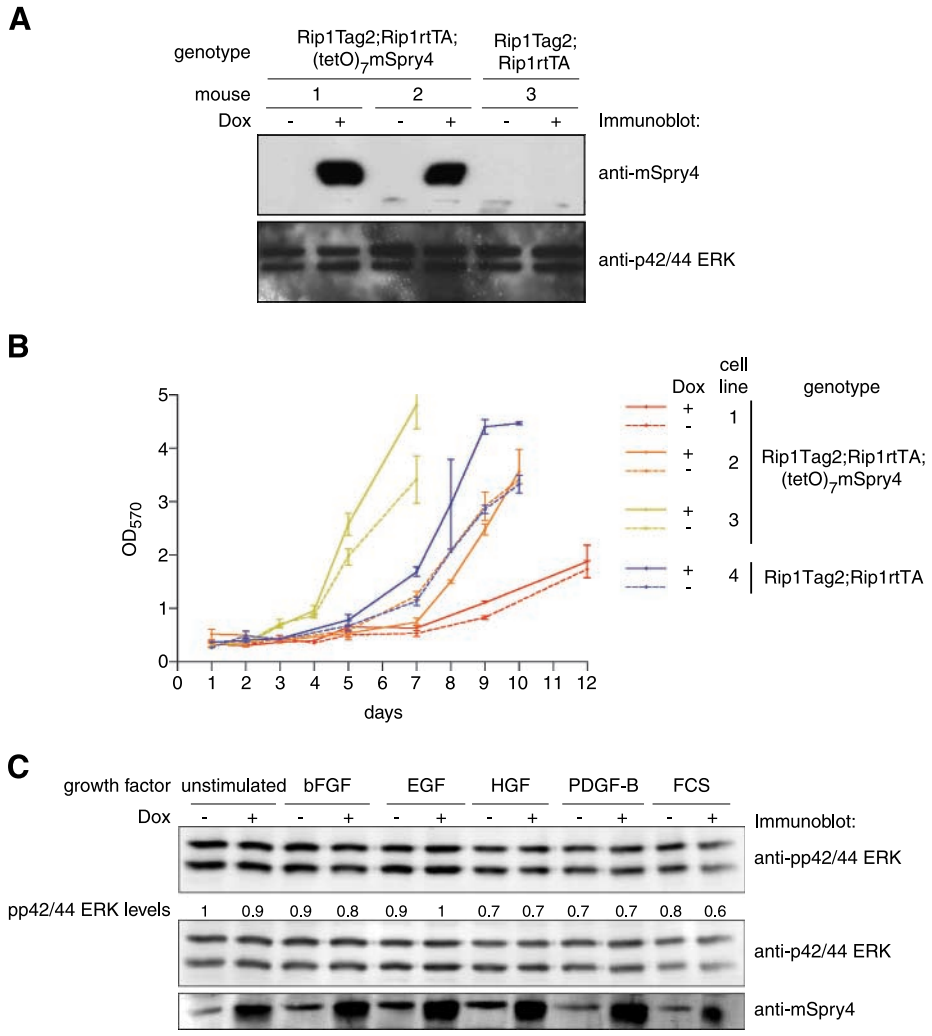

FIGURE 6. Inducible expression of mSpry4 in β tumor cell lines. **A.** Inducible mSpry4 expression. Tumor cell lines isolated from Rip1Tag2;Rip1rtTA and Rip1Tag2;Rip1rtTA;(tetO)$_7$mSpry4 mice were treated with doxycycline for 2 d. Lysates were resolved by SDS-PAGE and resulting immunoblots were sequentially probed with anti-mSpry4 antisera and antibodies against p42/44 ERK as loading control. The immunoblot shown is representative of three independent experiments. **B.** Cell proliferation. Tumor cell lines established from tumors of three different Rip1Tag2;Rip1rtTA;(tetO)$_7$mSpry4 mice and one Rip1Tag2;Rip1rtTA mouse were grown with (*continuous line*) or without (*dashed line*) doxycycline-induced mSpry4 expression. **C.** Growth factor stimulation. Cultured β tumor cells treated with doxycycline for 24 h were starved overnight and then stimulated for 30 min with FGF2, EGF, hepatocyte growth factor (HGF), platelet-derived growth factor-B (PDGF-B), or incubated in medium supplemented with 10% FCS as indicated. Lysates were resolved by SDS-PAGE and the resulting immunoblots were sequentially probed with the antibodies indicated. Levels of phospho-p42/44 ERK were normalized against total p42/44 ERK levels.

islets of Langerhans. Inducible expression of transgenic mSpry4 in β cells substantially changes islet morphology. Islets expressing mSpry4 in β cells are smaller in size, contain more α cells per islet area, and exhibit a defect in the sorting of α and β cells to the islet periphery and center, respectively. We tested several ways to explain these alterations caused by the ectotopic expression of mSpry4 in β cells. mSpry4 in β cells may affect signaling pathways underlying cell fate decisions, for example by repressing β-cell and favoring α-cell differentiation. Indeed, the expression of a dominant-negative version of FGFR1 in β cells has resulted in a net loss of insulin-positive cells without increasing β-cell apoptosis (39). These authors propose an autocrine loop of FGF signaling that might be involved in terminal differentiation and/or maturation of β cells. Our immunofluorescence microscopy analysis of pancreata of Rip1rtTA;(tetO)$_7$mSpry4 mice reveals that the mSpry4 transgene and the endogenous insulin gene are rarely coexpressed in the same cell and, if so, that insulin levels in these cells are clearly decreased (Fig. 2F-K; Table 1). Based on these results, we hypothesize that mSpry4 might interfere with FGF-mediated β cell maturation. However, in the dominant-negative FGFR1 neonates, neither islet organization nor the number of α cells have been affected, indicating that inhibition of FGFR1 signaling is not sufficient to explain the phenotype observed by the inducible expression of mSpry4 in developing β cells of Rip1rtTA;(tetO)$_7$mSpry4 embryos and newborn mice.

Also, mSpry4 could affect migration and aggregation of endocrine cells during development. Induction of precursor cell migration via FGFRs has been suggested to occur during pancreas development in rats (36, 42). However, although Spry proteins are mainly known for their repressive functions on the Ras/Raf/p42/44 ERK pathway, our experiments with PANC-1 cells suggest that mSpry4 inhibits cell adhesion and movement

TABLE 5. Expression of mSpry4 Expression Does Not Affect β-Tumor Cell Tumorigenicity

	−Dox	+Dox
Tumors/flank injected	5/8	4/8
Volume/tumor (mm^3)	220.9 ± 117.4	240.4 ± 185.7
*P**	0.9324	

NOTE: Values represent mean ± SD.
*P value of control vs doxycycline-treated animals (two-tailed Student's t test).

by a mechanism that does not affect the p42/44 ERK activation status (Fig. 3). Previously, it has been reported that Spry proteins are able to affect cell migration by inhibiting the activation of the small GTPase Rac1 (15, 26, 33). Moreover, mSpry2 expression leads to a relocalization and thereby to an enhanced activation of PTP1B that, in turn, dephosphorylates and inhibits the Rac1 activator p130Cas (27). In PANC-1 cells, we observed a shift in PTP1B localization from structures resembling the endoplasmic reticulum and focal adhesion sites in the absence of mSpry4 expression to a cytosolic localization in the presence of mSpry4 (Fig. 4). Despite numerous attempts, we have been unable to show a direct interaction between Spry2 or Spry4 with either the wild-type or a substrate-trapping (D181) form of PTP1B under stimulatory conditions (data not shown). PTP1B is known to repress cell migration and adhesion by interfering with integrin signaling, but conflicting models exist for the exact mechanism of PTP1B function (59, 60, 63). However, it is interesting to note that mice lacking the *β_1 integrin* gene specifically in β cells recapitulate the α-/β-cell sorting phenotype observed by the β cell–specific expression of mSpry4 (64), suggesting that integrin signaling may indeed play a critical role in islet cell segregation.

An identical cell sorting phenotype of the endocrine pancreas has also been described in mice lacking the cell adhesion molecule NCAM or in transgenic mice expressing a dominant-negative version of E-cadherin specifically in β cells (54, 65). Differences in cell adhesion capabilities in two motile cell types can serve as a driving force for segregation and sorting of these cell types, whereby less cohesive cells surround a core of more cohesive cells (58). Here, we show that mSpry4 inhibits matrix adhesion and migration of cells (Fig. 3A and B). Hence, the expression of endogenous mSpry4 in α cells might establish a difference in cohesiveness of α versus β cells and thereby affect islet cell segregation and the maintenance of islet organization. In contrast, transgenic expression of mSpry4 in β cells of Rip1rtTA;$(tetO)_7$mSpry4 mice compromises such differences in adhesion and migration, resulting in the observed islet cell sorting phenotype.

Both the loss of NCAM (54) and the loss of β_1 integrin function (64) mimic the islet cell sorting phenotype caused by the β cell–specific expression of mSpry4. Previously, we have reported that NCAM binds and activates FGFR in an FGF-independent manner, thereby activating the Ras/Raf/p42/44 ERK pathway, which leads to β_1 integrin–mediated cell adhesion and migration (66). The inhibition of cell adhesion and migration by mSpry4 reported here is thus consistent with the mSpry4-mediated repression of the FGFR signaling pathway. Yet, our results suggest that mSpry4 may act downstream of p42/44 ERK activation, possibly by modulating the subcellular localization and activity of PTP1B (see above) and/or by additional mechanisms remaining to be explored. Additionally, it has been reported that homotypic cell-cell contact of β cells influences insulin production, suggesting that the organization of β cells in the core of the islet is crucial for correct islet function (67, 68). The perturbed α- and β-cell localization, together with the reduced islet size and reduced insulin staining in mice expressing mSpry4 in β cells, does not interfere with blood glucose homeostasis as revealed by glucose tolerance tests (Supplementary Fig. S1).

We report here that mSpry4, when expressed in untransformed β cells, causes a significant phenotype in the developing pancreas. On the other hand, in Rip1Tag2 mice, where β cells are transformed by SV40 large T antigen, the effect of transgenic mSpry4 is less pronounced. The presence of mSpry4 leads only to a modest decrease in tumor size (Table 3), which is most likely due to slightly reduced tumor cell proliferation. This notion, together with the observation that mSpry4 has a heterogeneous effect on ERK activation and that larger tumors seem to negatively select against mSpry4 expression (Fig. 5), suggests that transformed β cells are not completely refractory to mSpry4 function. However, the effects of mSpry4 on β-cell carcinogenesis in Rip1Tag2 mice are minor and not significant probably due to the inclusion in the analysis of tumors with heterogeneous, low, or no expression of mSpry4. That transformed β cells are refractory to mSpry4 is further confirmed by experiments with β tumor cell lines established from Rip1Tag2;Rip1rtTA;$(tetO)_7$mSpry4 mice: Their proliferation, their activation of p42/44 ERK by different growth factors, and their tumorigenicity in transplanted mice are not at all affected by mSpry4 (Fig. 6; Table 5). Selection against transgene expression during Rip1Tag2 tumorigenesis is not without precedent: β cell–specific expression of a stabilized form of β-catenin also decreased during tumor progression (69). Transcriptional silencing is the most likely process by which these transgenes are being selected against in large β-cell tumors of Rip1Tag2 mice.

Whereas the modulatory function of Spry proteins on RTK-mediated signaling pathways has been extensively studied, their roles in carcinogenesis has only recently begun to be addressed. Gene expression surveys have revealed that Spry1 and Spry2 are down-regulated during the etiology of several cancer types, including cancers of the breast, prostate, and liver and melanoma (3, 43-46). Apparently, tumors seek to ablate the antagonistic activities of Spry proteins. However, high levels of expression of Spry2 in melanoma carrying the B-Raf V599E mutation and of Spry1 and Spry4 in gastrointestinal stromal tumors have been reported (3, 70). Finally, the data shown here suggest that besides selecting against the expression of Spry proteins, tumors can be resistant to the antagonistic function of Spry proteins. Accordingly, a number of transformed cell lines are not affected by the expression of any Spry isoform, regardless of the cancer type and the oncogenic transformation event (71).[5] Understanding the molecular basis of the acquisition of such resistance against Spry function as well as of the selection against Spry expression is certainly a key future task in the further design of therapeutic measures to interfere with RTK-mediated carcinogenesis.

Materials and Methods

Transgenic Mice

Rip1rtTA transgenic mice were generated according to standard procedures and have been described elsewhere (51). The mice express the reverse tetracycline transactivator under the control of the rat insulin promoter (Rip1). Rip1rtTA mice were crossed with transgenic $(tetO)_7$mSpry4 mice in which the

[5] Our unpublished results.

expression of murine Spry4 is driven by a promoter consisting of the reverse tetracycline transactivator binding element $(tetO)_7$ linked to an inactive cytomegalovirus minimal promoter $(tetO)_7$mSpry4 (32). Double-transgenic Rip1rtTA; $tet(O)_7$mSpry4 mice were crossed with Rip1Tag2 mice to generate the triple-transgenic Rip1Tag2;Rip1rtTA; $tet(O)_7$mSpry4 offspring. Generation and phenotypic characterization of Rip1Tag2 mice has been described previously (49). All mouse lines were strictly kept in a C57Bl/6 background. The PCR primers used for genotyping were as follows: Rip1rtTA, 5′-CATCTCAATGGCTAAGGCGTC-3′ and 5′-GACCAGCTACAGTCGGAAACC-3′; $(tetO)_7$mSpry4, 5′-CACCGGGACCGATCCAGC-3′ and 5′-GAAGTGCTGCTACTGCTGCTTA-3′; and Rip1Tag2, 5′-GGACAAACCACAACTAGAATGGCAG-3′ and 5′-CAGAGCAGAATTGTGGAGTGG-3′. All animal experimentations were in accordance with the guidelines of the Swiss Federal Veterinary Office and the regulations of the Cantonal Veterinary Office of Basel-Stadt.

Transgene Induction Experiments

Transgenic mSpry4 expression was induced by addition of doxycycline (1 mg/mL, Sigma Chemical Co.) to the drinking water in light-protected bottles. The water was replaced every second day. To express mSpry4 during embryogenesis, pregnant females were treated with doxycycline. Days of gestation were dated by detection of the vaginal plug. Double-transgenic Rip1rtTA;$tet(O)_7$mSpry4 and single-transgenic control littermates were sacrificed at 2 or 4 wk, respectively. Triple-transgenic tumor mice [Rip1Tag2;Rip1rtTA;$tet(O)_7$ mSpry4] were treated with doxycycline for 2 to 3 wk before sacrifice at the age of 7, 10, or 12 wk. Tumor incidence was determined macroscopically, and tumor volumes were calculated from the tumor diameter by assuming a spherical shape of the tumors.

Glucose Tolerance Test

Five-week-old double-transgenic Rip1rtTA;$tet(O)_7$mSpry4 and single-transgenic control littermates were starved overnight. After 12 h, 2 mg glucose (200 mg/mL diluted in PBS) per gram of body weight was injected into the tail vein. Blood glucose levels were measured every 30 min for 2 h using Accu-Check Sensor (Roche Diagnostics).

β Tumor Cell Injection into Nude Mice

Athymic nude-Fox-N1 nu/nu mice were obtained from Harlan Sprague-Dawley. β Tumor cells (1×10^6) positive for both Rip1rtTA and $(tetO)_7$mSpry4 transgenes were injected into the flanks of the mice. Mice were treated with doxycycline (1 mg/mL) in their drinking water from the day of injection or left untreated. Mice were sacrificed 6 wk after tumor cell injection.

Histology

Pancreata were fixed overnight at 4°C in 4% paraformaldehyde in PBS (pH 7.4) before processing and embedding in paraffin. Five-micrometer thick sections were cut for immunohistochemical analysis. For BrdUrd labeling, mice were injected i.p. with 100 mg BrdUrd (Sigma) per gram of body weight 2 h before tumor isolation. Rabbit sera against mSpry4 peptides were generated as previously described (71) and used for immunohistochemical and immunofluorescent analysis of mSpry4 expression. The following additional antibodies were used: guinea pig anti-insulin (DakoCytomation), goat anti-human glucagon (Santa Cruz Biotechnology), and biotinylated mouse anti-BrdUrd (Zymed). Antibody specificity was confirmed by incubating pancreatic sections without primary antibody or with preimmune sera.

Apoptotic cells were visualized with the *in situ* Cell Death Detection kit for peroxidase (Roche). All biotinylated secondary antibodies (Vector) were used at a 1:200 dilution, and positive staining was visualized with the ABC horseradish peroxidase kit and 3-amino-9-ethylcarbazole substrate kit for peroxidase (Vector) according to the manufacturer's instructions. For the analysis of tissue morphology, slides were counterstained with hematoxylin.

For immunofluorescence analysis, Alexa Fluor 568– and Alexa Fluor 488–labeled secondary antibodies diluted 1:200 were used (Invitrogen). For nuclear counterstain, 6-diamidino-2-phenylindole (Sigma) was used. For quantitation of proliferation (BrdUrd incorporation) and apoptosis (TUNEL reaction), the numbers of nuclei staining positive for BrdUrd or the TUNEL reaction were determined in 7 to 10 comparable fields per section with a ×40 objective, and the mean of positive cells ± SD per field was calculated. Blind analyses of insulin and glucagon double stainings were used to group mice in doxycycline-induced Rip1rtTA;tetOmSpry4 transgenics and control littermates. The areas of mSpry4- and insulin-expressing cells in tumors and islets were quantified by ImageJ software (ImageJ).

Cell Culture

PANC-1 cells were obtained from the American Tissue Culture Collection. For the generation of tumor cell lines, Rip1Tag2 mice carrying one or both of the transgenes Rip1rtTA and $tet(O)_7$mSpry4 were sacrificed at the age of 12 wk. Pancreatic tumors were isolated using a dissecting microscope, and tumor cell lines were established as described previously (72). All cells were maintained at 37°C with 5% CO_2 and cultured in high glucose DMEM, containing 10% fetal bovine serum and 2 mmol/L glutamine. Doxycycline (2 μg/mL) was added to normal medium to induce mSpry4 expression in tumor cells.

For proliferation assays, cell numbers were determined using a 3-(4,5-dimethylthiazol-2-yl)-2,5-diphenyltetrazolium bromide (MTT) assay. In brief, at t_0, 1×10^5 β tumor cells were seeded onto 24-well plates. Every 24 h, MTT (Sigma) was added to the cells at 0.5 mg/mL and incubated at 37°C for 90 min. Cells were solubilized in 500 μL of 95% isopropanol, 5% formic acid. Absorption of the solution was determined at 570 nm.

For cell migration assays, PANC-1 cells (3×10^4 per well) were seeded onto 8-μm pore size Transwell membranes (BD Biosciences) and incubated with medium without sera or medium supplemented with either 10% FCS or 100 ng/mL FGF2 in the lower or upper chamber as indicated. After 4.5 h, cells on top of the membranes were removed with sterile cotton swabs; membranes were fixed with 4% paraformaldehyde for 15 min at room temperature and stained with crystal violet (0.5% in 20% methanol, Sigma) for 20 min at room temperature. Labeled cells that had migrated through the membrane

were counted using a ×20 objective on a Zeiss microscope (Zeiss).

Matrix adhesion assays were done as previously described (66). Ninety-six–well plates were left uncoated or coated with 5 μg/cm^2 of mouse collagen IV (BD Biosciences) according to the manufacturer's recommendation, and PANC-1 cells (5×10^4 per well) were seeded and incubated for 2.5 h. Nonadherent cells were removed by washing with PBS. Adherent cells were fixed for 20 min with 25% glutaraldehyde, stained with crystal violet, and solubilized with 10% acetic acid. Absorbance was measured at 595 nm.

Adenoviral constructs encoding the mouse Spry4 cDNA (AdmSpry4) and the firefly luciferase cDNA (AdLite) were generated as described previously (73). Viral quantities were based on protein content using the conversion of 1 mg viral protein = 3.4×10^{12} virus particles. For viral infection of PANC-1 cells, culture medium was replaced with starvation medium (DMEM, 2 mmol/L glutamine) containing 2,500 virus particles per cell. After 5 h, the medium was replaced with fresh growth medium for another 5 h before overnight starvation and stimulation with growth factors the following day. PANC-1 and β tumor cells were stimulated for 30 min by the addition of recombinant human FGF2 (50 ng/mL), epidermal growth factor (50 ng/mL), hepatocyte growth factor (20 ng/mL), or platelet-derived growth factor (30 ng/mL; Catalys AG/Promega or Sigma).

Immunoblotting

PANC-1 and β tumor cells were lysed for 30 min on ice in lysis buffer [1% Triton X-100, 160 mmol/L NaCl, 20 mmol/L Tris (pH 8.0), 2 mmol/L Na_3VO_4, 10 mmol/L NaF and a 1:200 dilution of stock protease inhibitor cocktail for mammalian cells (Sigma)]. Tumor tissue samples were pooled and lysed in tissue lysis buffer [0.5% Triton X-100, 100 mmol/L NaCl, 2.5 mmol/L EDTA, and 10 mmol/L Tris (pH 8.0)]. Protein concentration was determined using a modified Bradford protocol (Bio-Rad Protein Assay; Bio-Rad Laboratories). Equal amounts of protein were dissolved in SDS-PAGE loading buffer and resolved by 12% SDS-PAGE. SDS-PAGE gels were transferred to polyvinylidene fluoride (Millipore) by semidry transfer in Towbin's buffer (20% methanol, 25 mmol/L Tris, 192 mmol/L glycine), blocked with either 4% bovine serum albumin or 5% skim milk powder in TBS with 0.05% Tween 20 (TBST). Primary and secondary antibodies were diluted in 4% bovine serum albumin or 5% skim milk powder in TBST. The following primary antibodies were used: mouse monoclonal anti-phosphorylated p42/44 ERK (Sigma), rabbit polyclonal anti-p42/44 ERK (Sigma), goat polyclonal anti-actin (Santa Cruz Biotechnology), and mouse monoclonal anti-PTP1B (BD Biosciences). Expression of mSpry4 was analyzed using rabbit sera against mSpry4 peptide as previously described (71). The following secondary antibodies conjugated to horseradish peroxidase were used: goat anti-mouse IgG (Sigma or Jackson Immunoresearch), rabbit anti-goat IgG (Sigma), and donkey anti-rabbit IgG (Amersham or Jackson Immunoresearch). Detected antibodies were visualized using enhanced chemiluminescence (GE Health Sciences/Amersham Biosciences or Interchim). In some cases, immunoblots were also visualized and quantitated using an Odyssey Imager (Li-Cor Biotechnology). In these cases, the following secondary antibody conjugates were used: goat anti-mouse Alexa 680 (Invitrogen) and goat anti-rabbit IRDye 800 (Rockland Immunochemicals).

Immunofluorescence

PANC-1 cells were plated on uncoated coverslips or on coverslips coated with 5 μg/cm^2 of mouse collagen IV (BD Bioscience). After 24 h, cells were fixed using 4% paraformaldehyde for 15 min at 37°C. Cells were permeabilized with cold 0.1% Triton X-100 in PBS for 10 min at 4°C. Then, cells were blocked in 4% goat serum in PBS for 1 h at room temperature. Anti-PTP1B antibody (BD Biosciences) was diluted 1:100 in 4% goat serum and incubated overnight at 4°C. Alexa 488–conjugated anti-mouse IgG and Alexa 568–conjugated anti-phalloidin antibodies (Molecular Probes) were diluted 1:200 in 4% goat serum. Nuclei were stained with 1 μg/mL 6-diamidino-2-phenylindole (Sigma) for 10 min at room temperature.

Statistical Analysis

Statistical analyses were done using GraphPad Prism software (GraphPad Software, Inc.).

Acknowledgments

We thank K. Strittmatter, H. Antoniadis, and U. Schmieder for technical support.

References

1. Mason JM, Morrison DJ, Basson MA, Licht JD. Sprouty proteins: multifaceted negative-feedback regulators of receptor tyrosine kinase signaling. Trends Cell Biol 2006;16:45–54.

2. Rubin C, Gur G, Yarden Y. Negative regulation of receptor tyrosine kinases: unexpected links to c-Cbl and receptor ubiquitylation. Cell Res 2005;15:66–71.

3. Lo TL, Fong CW, Yusoff P, et al. Sprouty and cancer: the first terms report. Cancer Lett 2006;242:141–50.

4. Hacohen N, Kramer S, Sutherland D, Hiromi Y, Krasnow MA. Sprouty encodes a novel antagonist of FGF signaling that patterns apical branching of the *Drosophila* airways. Cell 1998;92:253–63.

5. Casci T, Vinos J, Freeman M. Sprouty, an intracellular inhibitor of Ras signaling. Cell 1999;96:655–65.

6. Tefft JD, Lee M, Smith S, et al. Conserved function of mSpry-2, a murine homolog of *Drosophila* sprouty, which negatively modulates respiratory organogenesis. Curr Biol 1999;9:219–22.

7. de Maximy AA, Nakatake Y, Moncada S, Itoh N, Thiery JP, Bellusci S. Cloning and expression pattern of a mouse homologue of *Drosophila* sprouty in the mouse embryo. Mech Dev 1999;81:213–6.

8. Minowada G, Jarvis LA, Chi CL, et al. Vertebrate Sprouty genes are induced by FGF signaling and can cause chondrodysplasia when overexpressed. Development 1999;126:4465–75.

9. Impagnatiello MA, Weitzer S, Gannon G, Compagni A, Cotten M, Christofori G. Mammalian sprouty-1 and -2 are membrane-anchored phosphoprotein inhibitors of growth factor signaling in endothelial cells. J Cell Biol 2001;152:1087–98.

10. Mason JM, Morrison DJ, Bassit B, et al. Tyrosine phosphorylation of Sprouty proteins regulates their ability to inhibit growth factor signaling: a dual feedback loop. Mol Biol Cell 2004;15:2176–88.

11. Taketomi T, Yoshiga D, Taniguchi K, et al. Loss of mammalian Sprouty2 leads to enteric neuronal hyperplasia and esophageal achalasia. Nat Neurosci 2005;8:855–7.

12. Basson MA, Akbulut S, Watson-Johnson J, et al. Sprouty1 is a critical regulator of GDNF/RET-mediated kidney induction. Dev Cell 2005;8:229–39.

13. Shim K, Minowada G, Coling DE, Martin GR. Sprouty2, a mouse deafness gene, regulates cell fate decisions in the auditory sensory epithelium by antagonizing FGF signaling. Dev Cell 2005;8:553–64.

14. Gross I, Morrison DJ, Hyink DP, et al. The receptor tyrosine kinase regulator

Sprouty1 is a target of the tumor suppressor WT1 and important for kidney development. J Biol Chem 2003;278:41420–30.

15. Lee CC, Putnam AJ, Miranti CK, et al. Overexpression of sprouty 2 inhibits HGF/SF-mediated cell growth, invasion, migration, and cytokinesis. Oncogene 2004;23:5193–202.

16. Lee SH, Schloss DJ, Jarvis L, Krasnow MA, Swain JL. Inhibition of angiogenesis by a mouse sprouty protein. J Biol Chem 2001;276:4128–33.

17. Leeksma OC, Van Achterberg TA, Tsumura Y, et al. Human sprouty 4, a new ras antagonist on 5q31, interacts with the dual specificity kinase TESK1. Eur J Biochem 2002;269:2546–56.

18. Sasaki A, Taketomi T, Kato R, et al. Mammalian Sprouty4 suppresses Ras-independent ERK activation by binding to Raf1. Nat Cell Biol 2003;5:427–32.

19. Wong ES, Fong CW, Lim J, et al. Sprouty2 attenuates epidermal growth factor receptor ubiquitylation and endocytosis, and consequently enhances Ras/ERK signalling. EMBO J 2002;21:4796–808.

20. Egan JE, Hall AB, Yatsula BA, Bar-Sagi D. The bimodal regulation of epidermal growth factor signaling by human Sprouty proteins. Proc Natl Acad Sci U S A 2002;99:6041–6.

21. Rubin C, Litvak V, Medvedovsky H, Zwang Y, Lev S, Yarden Y. Sprouty fine-tunes EGF signaling through interlinked positive and negative feedback loops. Curr Biol 2003;13:297–307.

22. Hall AB, Jura N, DaSilva J, Jang YJ, Gong D, Bar-Sagi D. hSpry2 is targeted to the ubiquitin-dependent proteasome pathway by c-Cbl. Curr Biol 2003;13:308–14.

23. Cabrita MA, Christofori G. Sprouty proteins: antagonists of endothelial cell signaling and more. Thromb Haemost 2003;90:586–90.

24. Christofori G. Split personalities: the agonistic antagonist Sprouty. Nat Cell Biol 2003;5:377–9.

25. Yigzaw Y, Cartin L, Pierre S, Scholich K, Patel TB. The C terminus of sprouty is important for modulation of cellular migration and proliferation. J Biol Chem 2001;276:22742–7.

26. Poppleton HM, Edwin F, Jaggar L, Ray R, Johnson LR, Patel TB. Sprouty regulates cell migration by inhibiting the activation of Rac1 GTPase. Biochem Biophys Res Commun 2004;323:98–103.

27. Yigzaw Y, Poppleton HM, Sreejayan N, Hassid A, Patel TB. Protein-tyrosine phosphatase-1B (PTP1B) mediates the anti-migratory actions of Sprouty. J Biol Chem 2003;278:284–8.

28. Furthauer M, Lin W, Ang SL, Thisse B, Thisse C. Sef is a feedback-induced antagonist of Ras/MAPK-mediated FGF signalling. Nat Cell Biol 2002;4:170–4.

29. Warburton D, Tefft D, Mailleux A, et al. Do lung remodeling, repair, and regeneration recapitulate respiratory ontogeny? Am J Respir Crit Care Med 2001;164:S59–62.

30. Klein OD, Minowada G, Peterkova R, et al. Sprouty genes control diastema tooth development via bidirectional antagonism of epithelial-mesenchymal FGF signaling. Dev Cell 2006;11:181–90.

31. Mailleux AA, Tefft D, Ndiaye D, et al. Evidence that SPROUTY2 functions as an inhibitor of mouse embryonic lung growth and morphogenesis. Mech Dev 2001;102:81–94.

32. Perl AK, Hokuto I, Impagnatiello MA, Christofori G, Whitsett JA. Temporal effects of Sprouty on lung morphogenesis. Dev Biol 2003;258:154–68.

33. Chi L, Itaranta P, Zhang S, Vainio S. Sprouty2 is involved in male sex organogenesis by controlling fibroblast growth factor 9-induced mesonephric cell migration to the developing testis. Endocrinology 2006;147:3777–88.

34. Pictet RL, Clark WR, Williams RH, Rutter WJ. An ultrastructural analysis of the developing embryonic pancreas. Dev Biol 1972;29:436–67.

35. Slack JM. Developmental biology of the pancreas. Development 1995;121:1569–80.

36. Elghazi L, Cras-Meneur C, Czernichow P, Scharfmann R. Role for FGFR2IIIb-mediated signals in controlling pancreatic endocrine progenitor cell proliferation. Proc Natl Acad Sci U S A 2002;99:3884–9.

37. Celli G, LaRochelle WJ, Mackem S, Sharp R, Merlino G. Soluble dominant-negative receptor uncovers essential roles for fibroblast growth factors in multi-organ induction and patterning. EMBO J 1998;17:1642–55.

38. Hart A, Papadopoulou S, Edlund H. Fgf10 maintains notch activation, stimulates proliferation, and blocks differentiation of pancreatic epithelial cells. Dev Dyn 2003;228:185–93.

39. Hart AW, Baeza N, Apelqvist A, Edlund H. Attenuation of FGF signalling in mouse β-cells leads to diabetes. Nature 2000;408:864–8.

40. Szebenyi G, Fallon JF. Fibroblast growth factors as multifunctional signaling factors. Int Rev Cytol 1999;185:45–106.

41. Kato S, Sekine K, FGF-FGFR signaling in vertebrate organogenesis. Cell Mol Biol (Noisy-le-grand) 1999;45:631–8.

42. Miralles F, Czernichow P, Ozaki K, Itoh N, Scharfmann R. Signaling through fibroblast growth factor receptor 2b plays a key role in the development of the exocrine pancreas. Proc Natl Acad Sci U S A 1999;96:6267–72.

43. Kwabi-Addo B, Wang J, Erdem H, et al. The expression of Sprouty1, an inhibitor of fibroblast growth factor signal transduction, is decreased in human prostate cancer. Cancer Res 2004;64:4728–35.

44. Lo TL, Yusoff P, Fong CW, et al. The ras/mitogen-activated protein kinase pathway inhibitor and likely tumor suppressor proteins, sprouty 1 and sprouty 2 are deregulated in breast cancer. Cancer Res 2004;64:6127–36.

45. McKie AB, Douglas DA, Olijslagers S, et al. Epigenetic inactivation of the human sprouty2 (hSPRY2) homologue in prostate cancer. Oncogene 2005;24:2166–74.

46. Tsavachidou D, Coleman ML, Athanasiadis G, et al. SPRY2 is an inhibitor of the ras/extracellular signal-regulated kinase pathway in melanocytes and melanoma cells with wild-type BRAF but not with the V599E mutant. Cancer Res 2004;64:5556–9.

47. Christofori G, Naik P, Hanahan D. A second signal supplied by insulin-like growth factor II in oncogene-induced tumorigenesis. Nature 1994;369:414–8.

48. Folkman J, Watson K, Ingber D, Hanahan D. Induction of angiogenesis during the transition from hyperplasia to neoplasia. Nature 1989;339:58–61.

49. Hanahan D. Heritable formation of pancreatic β-cell tumours in transgenic mice expressing recombinant insulin/simian virus 40 oncogenes. Nature 1985;315:115–22.

50. Perl AK, Wilgenbus P, Dahl U, Semb H, Christofori G. A causal role for E-cadherin in the transition from adenoma to carcinoma. Nature 1998;392:190–3.

51. Milo-Landesman D, Surana M, Berkovich I, et al. Correction of hyperglycemia in diabetic mice transplanted with reversibly immortalized pancreatic β cells controlled by the tet-on regulatory system. Cell Transplant 2001;10:645–50.

52. Apelqvist A, Ahlgren U, Edlund H. Sonic hedgehog directs specialised mesoderm differentiation in the intestine and pancreas. Curr Biol 1997;7:801–4.

53. Grapin-Botton A, Majithia AR, Melton DA. Key events of pancreas formation are triggered in gut endoderm by ectopic expression of pancreatic regulatory genes. Genes Dev 2001;15:444–54.

54. Esni F, Taljedal IB, Perl AK, Cremer H, Christofori G, Semb H. Neural cell adhesion molecule (N-CAM) is required for cell type segregation and normal ultrastructure in pancreatic islets. J Cell Biol 1999;144:325–37.

55. Herrera PL, Huarte J, Sanvito F, Meda P, Orci L, Vassalli JD. Embryogenesis of the murine endocrine pancreas; early expression of pancreatic polypeptide gene. Development 1991;113:1257–65.

56. Hardikar AA, Marcus-Samuels B, Geras-Raaka E, Raaka BM, Gershengorn MC. Human pancreatic precursor cells secrete FGF2 to stimulate clustering into hormone-expressing islet-like cell aggregates. Proc Natl Acad Sci U S A 2003;100:7117–22.

57. Hui H, Wright C, Perfetti R. Glucagon-like peptide 1 induces differentiation of islet duodenal homeobox-1-positive pancreatic ductal cells into insulin-secreting cells. Diabetes 2001;50:785–96.

58. Steinberg MS, Takeichi M. Experimental specification of cell sorting, tissue spreading, and specific spatial patterning by quantitative differences in cadherin expression. Proc Natl Acad Sci U S A 1994;91:206–9.

59. Liang F, Lee SY, Liang J, Lawrence DS, Zhang ZY. The role of protein-tyrosine phosphatase 1B in integrin signaling. J Biol Chem 2005;280:24857–63.

60. Cheng A, Bal GS, Kennedy BP, Tremblay ML. Attenuation of adhesion-dependent signaling and cell spreading in transformed fibroblasts lacking protein tyrosine phosphatase-1B. J Biol Chem 2001;276:25848–55.

61. Hernandez MV, Sala MG, Balsamo J, Lilien J, Arregui CO. ER-bound PTP1B is targeted to newly forming cell-matrix adhesions. J Cell Sci 2006;119:1233–43.

62. Crnic I, Strittmatter K, Cavallaro U, et al. Loss of neural cell adhesion molecule induces tumor metastasis by up-regulating lymphangiogenesis. Cancer Res 2004;64:8630–8.

63. Arregui CO, Balsamo J, Lilien J. Impaired integrin-mediated adhesion and signaling in fibroblasts expressing a dominant-negative mutant PTP1B. J Cell Biol 1998;143:861–73.

64. Kren A, Baeriswyl V, Lehembre F, et al. Increased tumor cell dissemination and cellular senescence in the absence of β(1)-integrin function. EMBO J 2007;26:2832–42.

65. Dahl U, Sjodin A, Semb H. Cadherins regulate aggregation of pancreatic β-cells *in vivo*. Development 1996;122:2895–902.

66. Cavallaro U, Niedermeyer J, Fuxa M, Christofori G. N-CAM modulates tumour-cell adhesion to matrix by inducing FGF-receptor signalling. Nat Cell Biol 2001;3:650–7.

67. Bosco D, Orci L, Meda P. Homologous but not heterologous contact increases the insulin secretion of individual pancreatic β-cells. Exp Cell Res 1989;184:72–80.

68. Philippe J, Giordano E, Gjinovci A, Meda P. Cyclic adenosine monophosphate prevents the glucocorticoid-mediated inhibition of insulin gene expression in rodent islet cells. J Clin Invest 1992;90:2228–33.

69. Herzig M, Savarese F, Novatchkova M, Semb H, Christofori G. Tumor progression induced by the loss of E-cadherin independent of β-catenin/Tcf-mediated Wnt signaling. Oncogene 2007;26:2290–8.

70. Linn SC, West RB, Pollack JR, et al. Gene expression patterns and gene copy number changes in dermatofibrosarcoma protuberans. Am J Pathol 2003;163:2383–95.

71. Cabrita MA, Jaggi F, Widjaja SP, Christofori G. A Functional Interaction between Sprouty Proteins and Caveolin-1. J Biol Chem 2006;281:29201–22912.

72. Efrat S, Linde S, Kofod H, et al. β-Cell lines derived from transgenic mice expressing a hybrid insulin gene-oncogene. Proc Natl Acad Sci U S A 1988;85:9037–41.

73. Michou AI, Lehrmann H, Saltik M, Cotten M. Mutational analysis of the avian adenovirus CELO, which provides a basis for gene delivery vectors. J Virol 1999;73:1399–410.

Molecular Cancer Research

Modulation of Endocrine Pancreas Development but not β -Cell Carcinogenesis by Sprouty4

Fabienne Jäggi, Miguel A. Cabrita, Anne-Karina T. Perl, et al.

Mol Cancer Res 2008;6:468-482.